Supporting Information for

Methacrylated Gelatin-embedded Fabrication of 3D Graphene-supported Co_3O_4 Nanoparticles for Water Splitting

Minghao Zhuang[1, 2§], Zhenjing Liu[1§], Yao Ding[1§], Gui-Liang Xu[2], Yuhui Li[3, 4], Abhishek Tyagi[1], Xiaoyi Zhang[5], Cheng-Jun Sun[5], Yang Ren[5], Xuewu Ou[1], Hoilun Wong[1], Yuting Cai[1], Ruizhe Wu[1], Irfan Haider Abidi[1], Qicheng Zhang[1], Feng Xu[3, 4], Khalil Amine[2, 6] and Zhengtang Luo[1*]

[1] *Department of Chemical and Biological Engineering, William Mong Institute of Nano Science and Technology and Hong Kong Branch of Chinese National Engineering Research Center for Tissue Restoration and Reconstruction, The Hong Kong University of Science and Technology, Clear Water Bay, Kowloon, Hong Kong*

[2] *Chemical Sciences and Engineering Division, Argonne National Laboratory, 9700 South Cass Avenue, Lemont, Illinois 60439, United States*

[3] *The Key Laboratory of Biomedical Information Engineering of Ministry of Education, School of Life Science and Technology, Xi'an Jiaotong University, Xi'an 710049, China*

[4] *Bioinspired Engineering and Biomechanics Center (BEBC), Xi'an Jiaotong University, Xi'an 710049, China*

[5] *X-ray Science Division, Advanced Photon Source, Argonne National Laboratory, 9700 South Cass Avenue, Lemont, Illinois 60439, United States*

[6] *Materials Science and Engineering, Stanford University, Stanford, CA 94305, United States*

§ M.H.Z., Z.J.L. and Y.D. contributed to this work equally

***E-mail:** keztluo@ust.hk (Z.T.L.)

Experimental Section

Methacrylated gelatin (GelMA) synthesis Methacrylated gelatin was synthesized based on previous work.[1] Briefly, 10 g gelatin powder (Sigma Aldrich) was mixed at 10 wt% into 100 ml deionized water at 50 ºC and stirred until fully dissolved. 0.8 ml/g methacrylic anhydride (MA) (Sigma Aldrich) was added drop by drop to the gelatin solution under stirred conditions at 50 ºC and allowed to react for 2.5 h. Following the mixture was dialyzed against deionized water for 1 week to remove methacrylic anhydride and other impurities. The solution was lyophilized for 1 week to generate a white porous foam and stored at -4 ºC for further use.

Preparation of 3D graphene foam (GF) The 3D graphene foam was synthesized with Ni foam (size is 1*1 cm^2 and pixels per inch (PPI) is 100) as template,[2] the Ni foam was chemical polished with the etchant solution (5g $FeCl_3$, 10 ml HCl and 100ml deionized water). The polish process was operated by immersing Ni foam into the solution located in a supersonic for 10-15s to remove impurities or native oxide on the surface. Then Ni foam was rinsed with deionized water for 3 times to remove etchant solvent residue. Finally, the foam was dried by nitrogen gas gun. Then APCVD (atmospheric pressure chemical vapor deposition) was applied in our growth of graphene. Nitrogen (Hong Kong Specialty Gases Co., LTD, 99.999%, oxygen concentration < 3 ppm) with flow rate of 300 sccm was used to expel air out of system for at least 15 minutes and then furnace was powered on to heat the substrate from room temperature to 900ºC. After growth temperature stable, hydrogen (Hong Kong Specialty Gases Co., LTD, 99.999%, oxygen concentration < 5 ppm) with flow rate of 100 sccm was introduced into system for 30 minutes annealing. Then, ethylene (Hong Kong Specialty Gases Co., LTD, 99.95%) with flow rate of 10 sccm was introduced to start growth for 5 min. Finally, powering off system and fast cooling was applied to cool down the system. The 3D graphene foam was got by firstly immersing Ni-graphene foam etchant solution (20g $FeCl_3$, 10 ml HCl and 200ml deionized water) for 12h to completely remove Ni scaffold, then rinsed by 0.01M HCl solution to remove the residual $FeCl_3$, followed by rinsing with running deionized water to get free-standing 3D graphene foam.

Absorption of photo initiator on graphene surface The photo initiator (2-hydroxy-2-methylpropiophenone, 97%, Sigma Aldrich) was adsorbed on graphene surface by immersing the graphene foam into 5 v% photo initiator/deionized water suspension for 0, 0.5, 1, 1.5 and 2h, then stored in deionized water for further use. The as prepared graphene foam/photo initiator composites with various modifying time were tested by Raman spectrometer. For AFM analysis, first we sonicated the graphene foam in 75% ethanol solution for 30 min, by dip-coating method, we made the graphene flakes sample on SiO_2/Si wafer, further tested the same position before and after immersing in 5 v% photo initiator/deionized water suspension for 1h.

Preparation of graphene-supported 3D porous GelMA The as prepared 3D graphene foam was soaked into as-prepared GelMA aqueous solution (1, 2, 3 wt%) with 5 v% photo initiator for 1h, then exposed under UV light (365 nm, 1.350 W/cm^2) for 5 min to obtain the graphene foam/GelMA hydrogel composites. The Ni foam/GelMA and Ni-graphene foam/GelMA composites were prepared in the same way by replacing the graphene foam by Ni foam and Ni-graphene foam.

Fabrication of monodispersed cobalt oxides nanoparticles on nitrogen-doped graphene Foam (Co_3O_4/NGF) with different sizes Immersing the as-prepared graphene-supported 3D porous GelMA into $CoCl_2$ aqueous solution with concentration of 0.02, 0.05, 0.1, 0.2 and 0.5 mol/L for 24h to reach absorption equilibrium. Then rinsed by 0.1 mol/L HCl and DI water for 3 times, respectively. Followed by freeze-drying process to obtain the lyophilized GelMA coated 3D graphene foam with $CoCl_2$ embedded in the polymer matrix, then address it in the furnace, heat it up to 500ºC by 5ºC/min under Ar (200 sccm), annealing at 500ºC for 30 min then naturally cool down to room temperature to obtain the final product, Co_3O_4/NGF.

***In operando* synchrotron HEXRD** *In operando* HEXRD was carried out by heating the $CoCl_2[H_2O]_2$@GelMA/GF precursor in a LINKAM TS-1500 furnace up to 580 °C with a heating rate of 5 °C min^{-1} in Ar atmosphere, and was conducted at sector 11-ID-D of the Advanced Photon Source (APS) at Argonne National Laboratory with a wavelength of 0.6525 Å. HEXRD patterns were continuously collected during the course of the experiment.

X-ray absorption near edge spectroscopy (XANES)/Extended X-ray absorption fine structure (EXAFS) XANES and EXAFS experiments on the Co K-edge of $CoCl_2[H_2O]_2$@GelMA/GF precursor and Co_3O_4/NGF were carried out in transmission mode at Beamline 20-BM-B of the APS.

Electrodes preparation and electrochemical measurements All the synthesized products were pretreated by DI water washing and freeze drying process. Electrochemical measurements were performed with an electrochemical workstation (CHI 760C, CH Instruments Inc.). Ag/AgCl electrode (saturated KCl) and a carbon bar were used as the reference and counter electrode, respectively. Typically for 3 nm size one, 5 cm * 5 cm of Co_3O_4/NGF catalyst was compressed on one piece of Ni foam with Co_3O_4 mass loading of 0.1 mg/cm^2. *(For other Co_3O_4/NGF with various sizes of Co_3O_4 nanoparticles, we made the mass loading of Co_3O_4 same as the 3-nm one for fair comparison)* HER and OER polarization curves were acquired by sweeping the potential from 0.1 to -0.6 V (vs RHE) for HER and from 1.1 to 1.9 V (vs RHE) for OER at a potential sweep rate of 1 mV/s in 1 M KOH, respectively. All polarization curves were NOT iR-corrected. Accelerated stability tests were performed at room temperature by potential cycling 0.1 to -0.6 V (vs RHE) for HER and from 1.1 to 1.9 V (vs RHE) for OER at a potential sweep rate of 50 mV/s for a given number of cycles. Current−time responses were operated for 25h. In all measurements, the Ag/AgCl reference electrode was calibrated with respect to a reversible hydrogen electrode (RHE). The calibration was performed in a high-purity N_2 saturated 0.1M $HClO_4$. Cyclic voltammograms (CVs) were collected at a scan rate of 1 mV/s, and the average of the two potentials at which the current crossed zero was taken as the thermodynamic potential for the hydrogen electrode reactions. Noted that E(RHE) = E(Ag/AgCl) + 0.3223 V. The electrochemical impedance spectroscopy (EIS) was carried out in the range from 100 K to 0.01 Hz with an AC amplitude of 10 mV. Overall water splitting studies were performed in a two-electrode system with Co_3O_4/NGF on Ni foam as both cathode and anode electrodes, the electrocatalytic activity of Co_3O_4/NGF electrodes towards the overall water splitting was examined by polarization curves using linear sweep voltammetry (LSV) in 1 M KOH with scan rate of 1 mV s^{-1}. For comparison, repeat the same process by replacing the Co_3O_4/NGF by NGF, GF, and pristine NiF substrate, respectively.

Computational modeling and simulations The structure of photo-initiator was parameterized in accordance with CGENFF,[3] using ParamCharm.[4] The penalties obtained were around 12, therefore can be implemented with some validation if required. The photo-initiator was placed 15 Å above the graphene sheet. The graphene sheet 50 x 50 Å was designed using Nanotube Builder plugin in VMD,[5] modeled using aromatic carbon atom with neutral charge, and the graphene sheet was fixed in X and Y axis. All the simulations were performed in NAMD2.10 [6] and CHARMM force field was adopted in our simulations. The photo initiator-graphene system energy minimized for 10000 ps (picoseconds), and equilibrated in NVT ensemble for 2 ns (nanoseconds), followed by production run implemented in NVT ensemble for 50 ns. Temperature and pressure was 300K and 1atm during simulations. The image rendering and analysis was performed by VMD.

Materials Characterization The microstructure and morphology of 3D graphene foam/GelMA and Co_3O_4/NGF samples were characterized by scanning electron microscope (SEM, JEOL 6390) and Transmission electron microscopy (TEM, JEOL 2010). The chemical information was examined by Fourier transform infrared spectroscopy (FTIR, Vertex 70 Hyperion 1000). The chemical composition and elemental valence states were characterized by X-ray photoelectron spectroscopy (XPS, PHI 5600). The Raman spectrum was recorded with a Renishaw Raman RM3000 scope using a 514 nm excitation argon laser. To characterize the crystal structure. Atomic Force Microscope (AFM, tapping model) was applied to investigate the height difference of graphene and photo initiator modified graphene surface, AFM was scanned under semi-contact mode using a NTEGRA probe NanoLaboratory (NT-MDT, Inc.) with ACTA tips from AppNano at 1.5 Hz scan rate and 512×512 resolution.

Supporting Figures

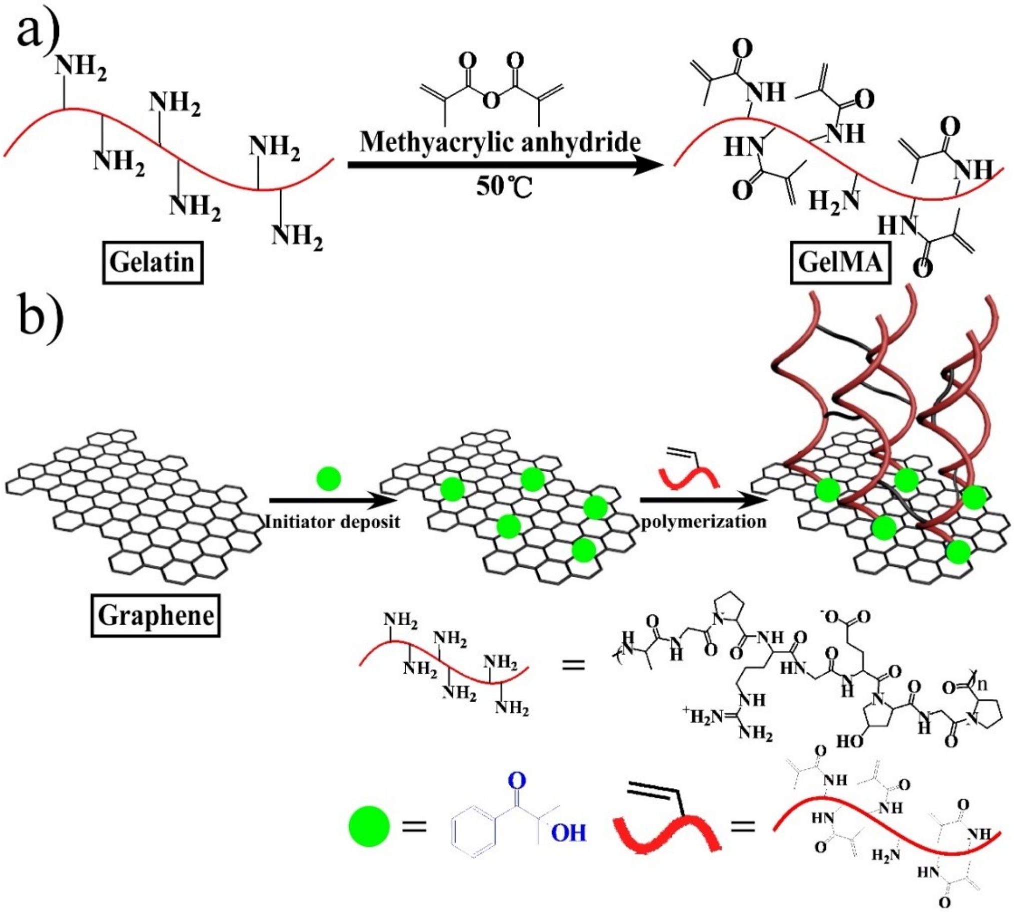

Figure S1. Schematic preparation of GelMA and GelMA/Graphene composite. a) Synthesis route of methacrylated gelatin (GelMA): Gelatin macromers containing amine groups are reacted with methacrylic anhydride (MA) to graft methacrylate groups. **b)** Fabrication process of non-covalently functionalized GelMA/Graphene composite. First, photo-initiator molecules deposit uniformly on the surface of graphene *via* π-π interaction; Second, UV assisted *in situ* polymerization of GelMA thin film on graphene surface.

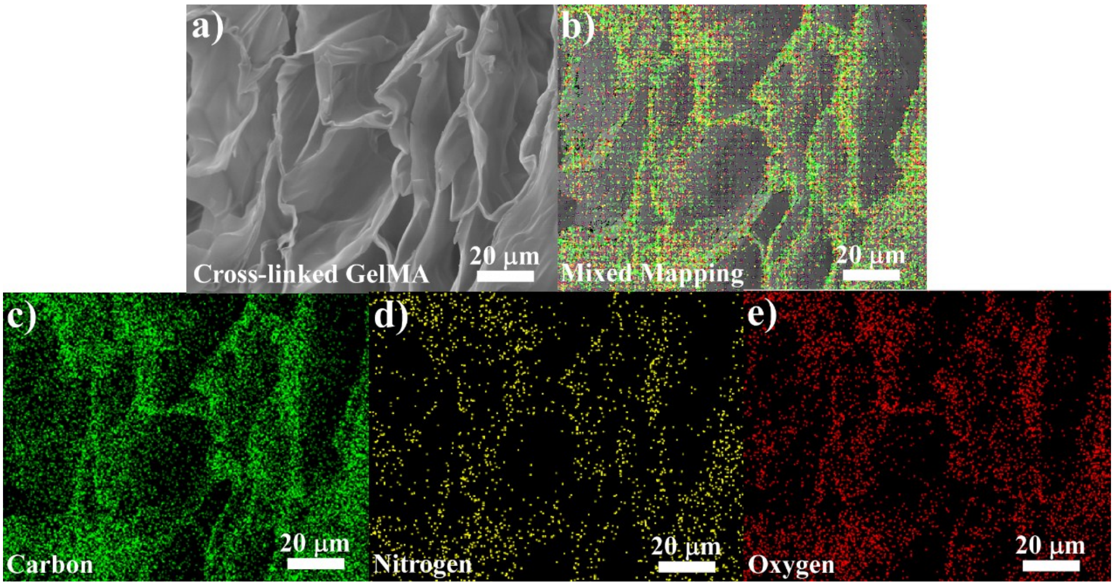

Figure S2. SEM images of cross-linked porous GelMA hydrogel. a) SEM image of lyophilized cross-linked GelMA hydrogel. **b)** Mixed elemental mapping image of panel a, followed by **c)** carbon, **d)** nitrogen and **e)** oxygen elemental mapping images.

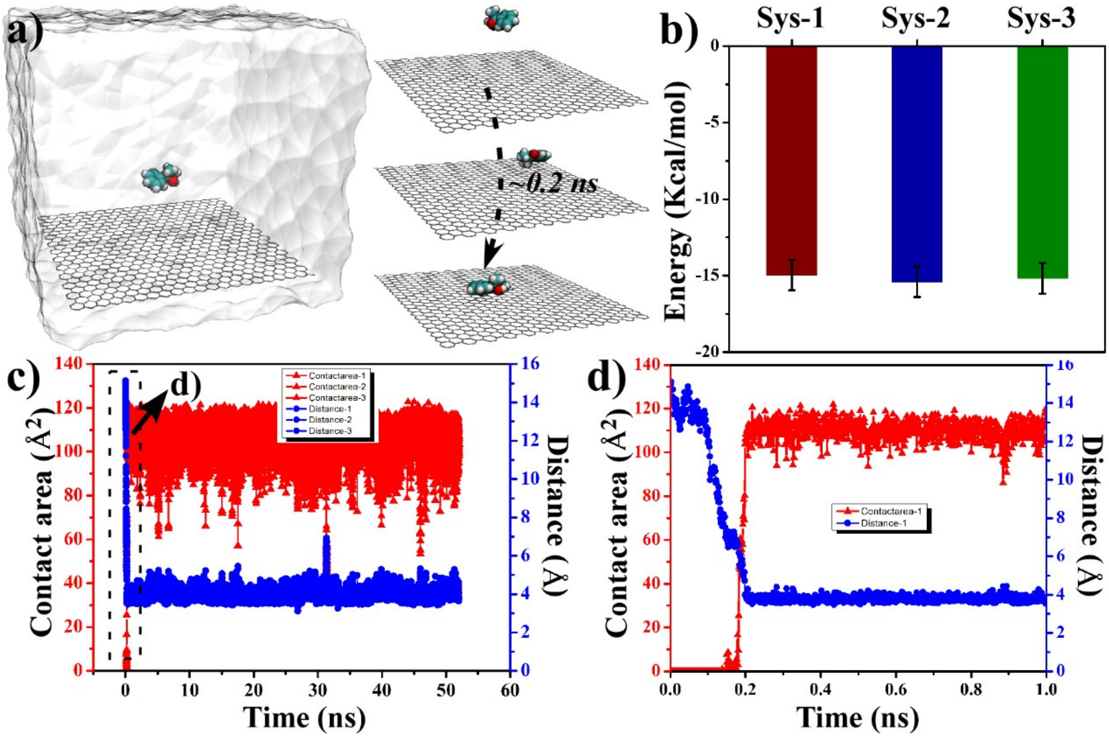

Figure S3. Adsorbing molecular dynamics simulations of photo-initiator on graphene. a) The photo-initiator placed above graphene in water (shown in transparent water box), after 0.2 ns photo-initiator adsorbed on graphene surface. **b)** vdW interaction energy of photo-initiator for three simulations with graphene, which is approximately -15 kcal/mol. **c)** The time evolution of contact area and center of mass (Distance) between photo-initiator and graphene for all the systems. **d)** For initial 1 ns of equilibration run.

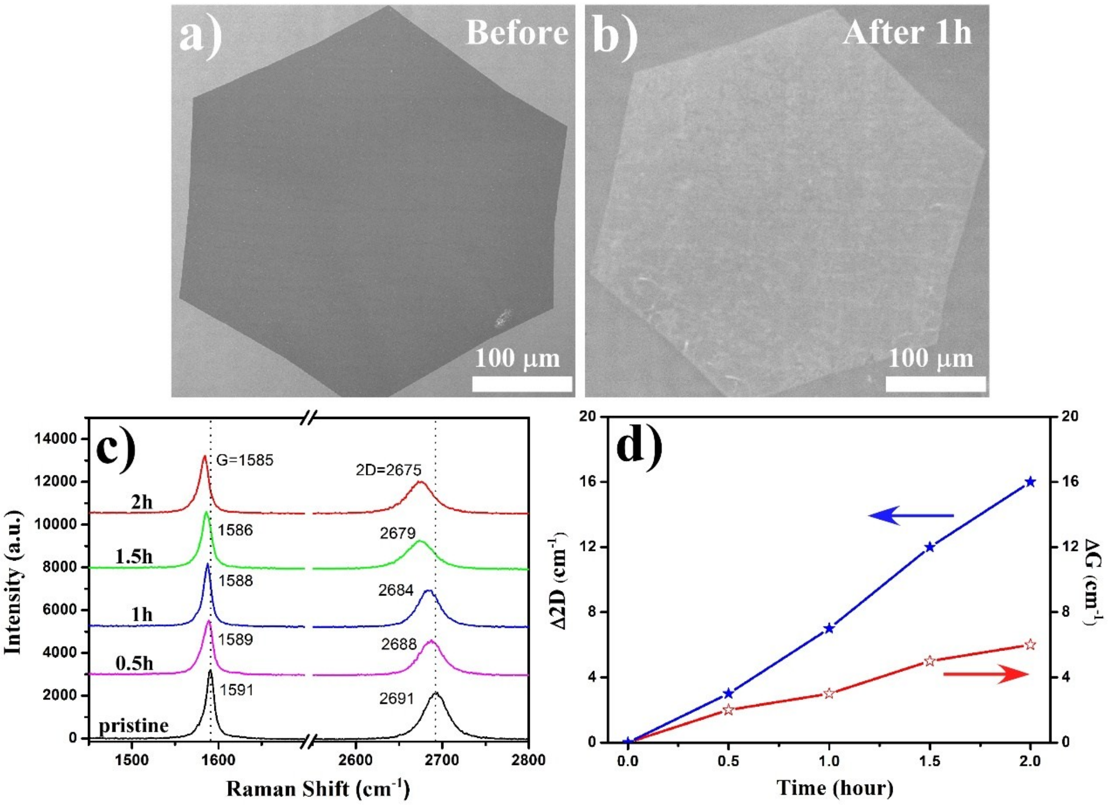

Figure S4. SEM and Raman spectra of pristine graphene and photo-initiator molecules doped graphene. a) SEM image of pristine CVD graphene and **b)** photo-initiator molecules doped graphene on silica wafer substrate, the different color contrast between hexagonal graphene area and outside in these two images illustrates that large amount of small molecules cover over the surface of graphene in b, which induce the charge concentrated in the hexagonal area rather than a. **c)** Raman spectra shifts of photo-initiator doped graphene foam with different immersing time (0, 0.5, 1, 1.5, 2h) in 0.5 v% photo-initiator/deionized water suspension. **d)** G and 2D peaks shifts of photo-initiator doped graphene foam, data derived from c.

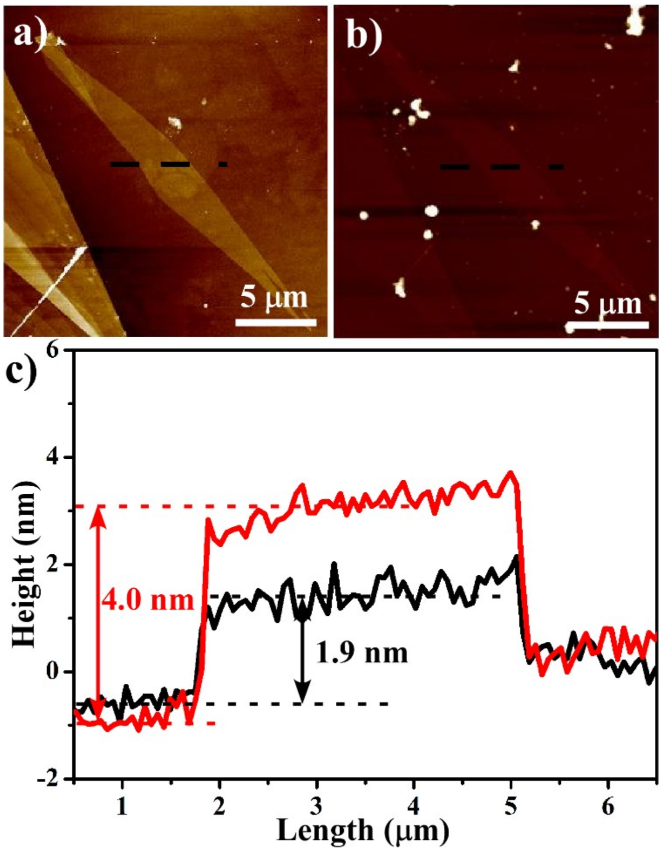

Figure S5. AFM images of pristine graphene and photo-initiator doped graphene on SiO$_2$/Si surface. a) Graphene debris and **b)** photo-initiator modified Graphene, the white particles are impurities. **c)** Height differences of graphene and photo-initiator doped graphene at the same position before (black) and after (red) photo-initiator molecules doping, corresponding to the marked dotted position in (a) and (b), respectively.

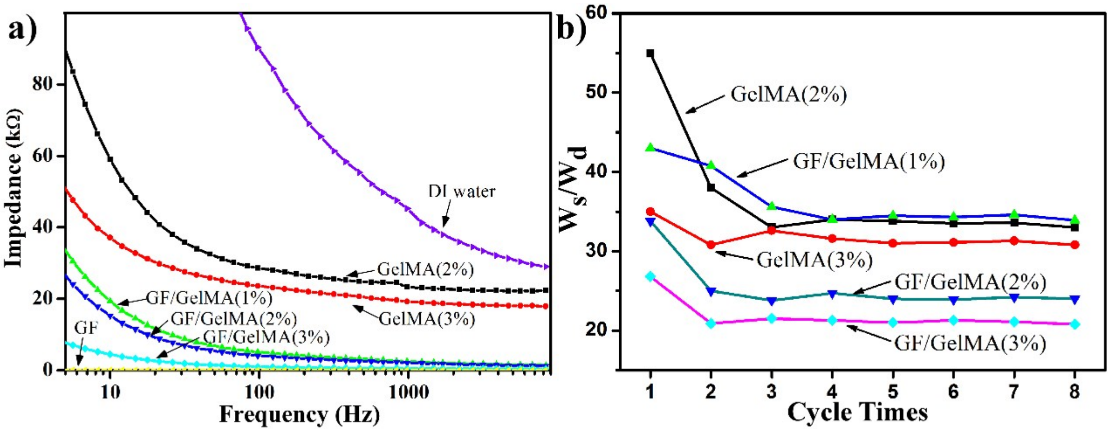

Figure S6. Electrochemical and water retention properties of GelMA/GF composites with different concentration of GelMA. a) Impedance curves of pure GelMA, pristine GF and GelMA/GF under 5 to 10^4 Hz with an AC amplitude of 10 mV. **b)** Water retention results of pure GelMA and GelMA/GF composites with various concentration at different cycle times. *(Here 1 wt% GelMA is too weak to maintain hydrogel state, we only tested for 2 and 3 wt%) and GelMA/GF (1, 2 and 3 wt%) in deionized water for 24h to fully swell, then recorded the weight as the 1st saturated weight (W_s). The samples were freeze-dried and then weighed again recording it as the 1st dehydration state weight (W_d). The freeze-drying and weighing process was repeated up to 8 times. The W_s /W_d ratio gives the value for the water retention ability of the samples.[7] The results show that GelMA/GF (1 wt%) has the best water retention performance with a largest value of 34 for its W_s/W_d. The GelMA/GF with 2 wt% and 3 wt% also gave large values of 25 and 20, respectively.)*

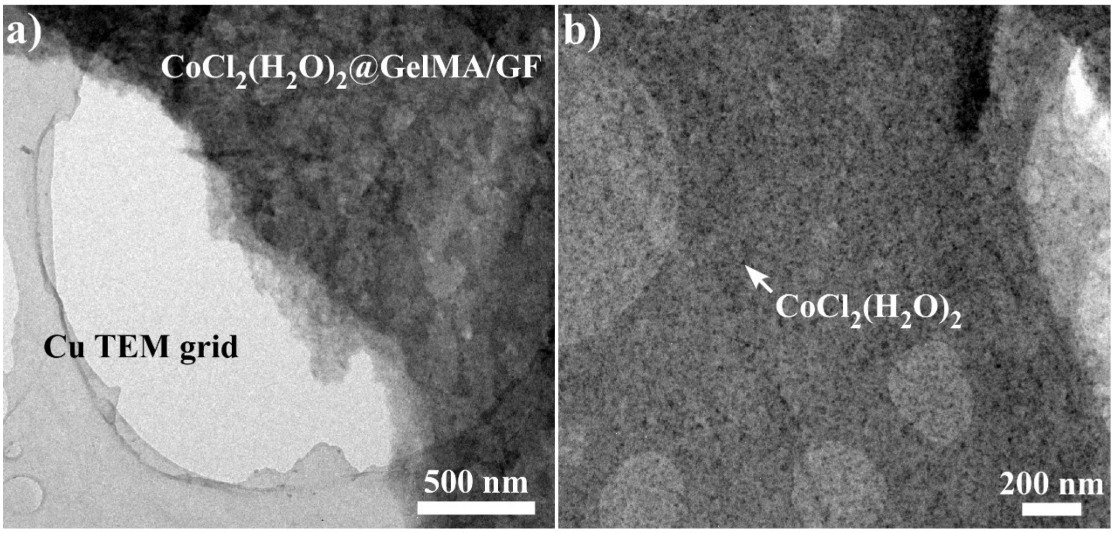

Figure S7. TEM images of $CoCl_2(H_2O)_2$@GelMA/GF. a) Overview of $CoCl_2(H_2O)_2$@GelMA/GF flakes on Cu TEM grid. **b)** High-resolution image of $CoCl_2(H_2O)_2$@GelMA/GF, the amorphous substrate is GelMA/GF matrix, the uniformly dispersed dark dots are the crystalline $CoCl_2[H_2O]_2$.

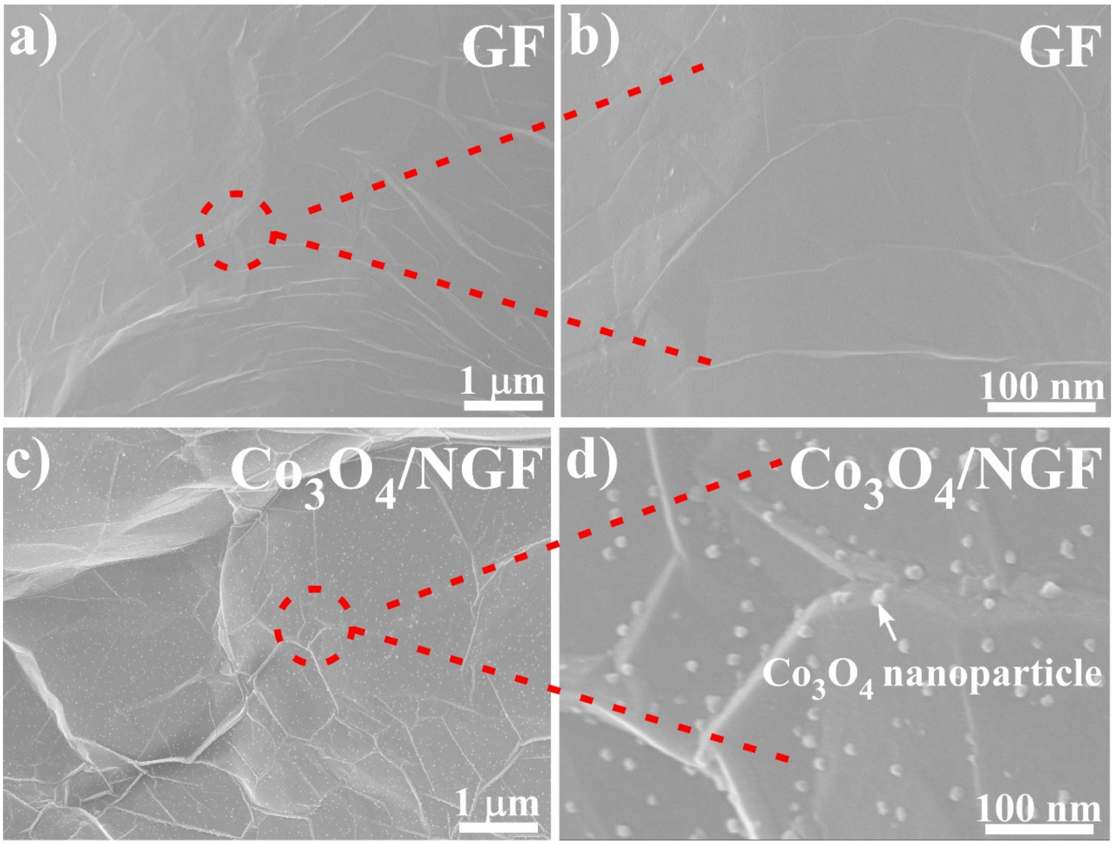

Figure S8. SEM results of Co_3O_4/NGF composite and its control sample. Low and high resolution SEM images of **a, b)** GF and **c, d)** Co_3O_4/NGF after same fabrication route by applying pristine GF and GelMA/GF as template, respectively.

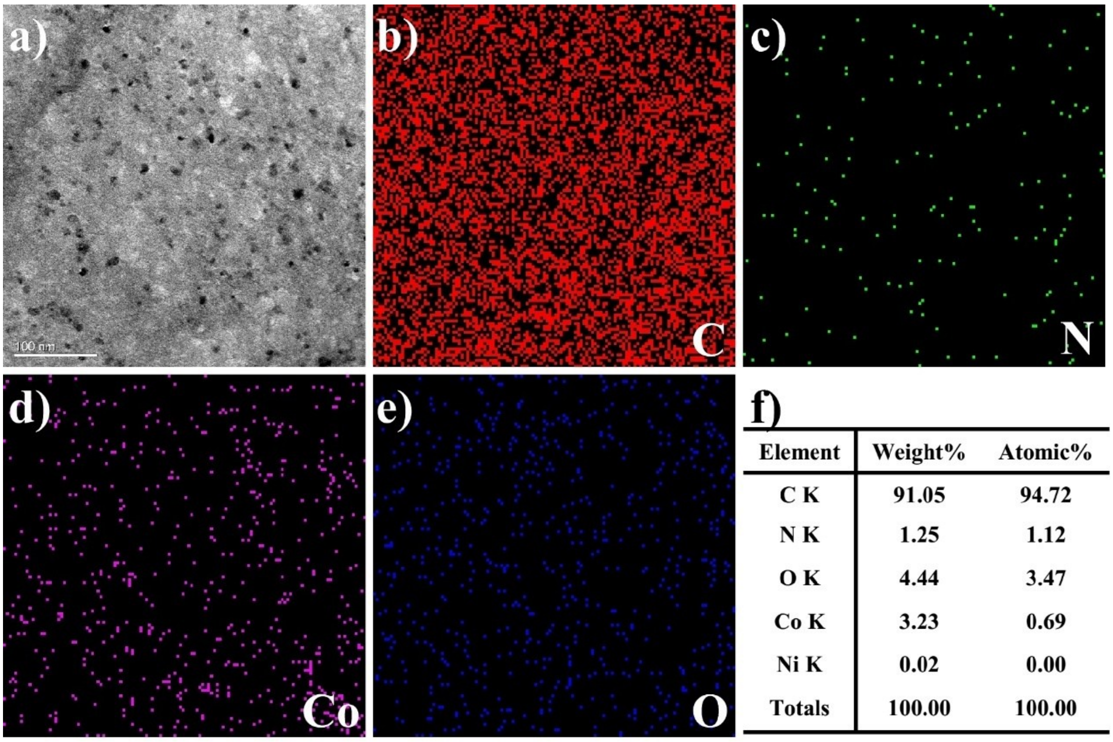

Element	Weight%	Atomic%
C K	91.05	94.72
N K	1.25	1.12
O K	4.44	3.47
Co K	3.23	0.69
Ni K	0.02	0.00
Totals	100.00	100.00

Figure S9. TEM elemental mapping results of Co_3O_4/N-doped Graphene Foam (Co_3O_4/NGF). a) TEM image of Co_3O_4/NGF, **b)** C, **c)** N, **d)** Co and **e)** O elemental mapping images of NGF. **f)** Followed by the summary of C, N, Co, O and Ni element content in Co_3O_4/NGF. (Ni element is too low to form a clear mapping result, the content data is extracted from the overall elemental spectrum.)

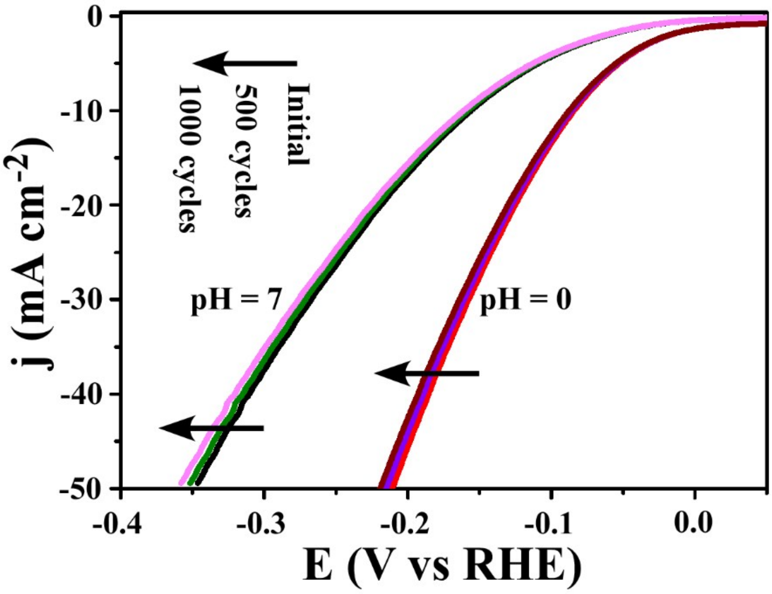

Figure S10. Catalytic activity and long-term stability characterization of Co_3O_4/NGF in 0.5M H_2SO_4 (pH ~ 0) and 1M PBS buffer solution (pH ~ 7). The polarization curves of Co_3O_4/NGF (Co_3O_4 nanoparticles size ~3 nm) with various CV cycles and steady-state current density as a function of applied voltage in 1M KOH toward HER.

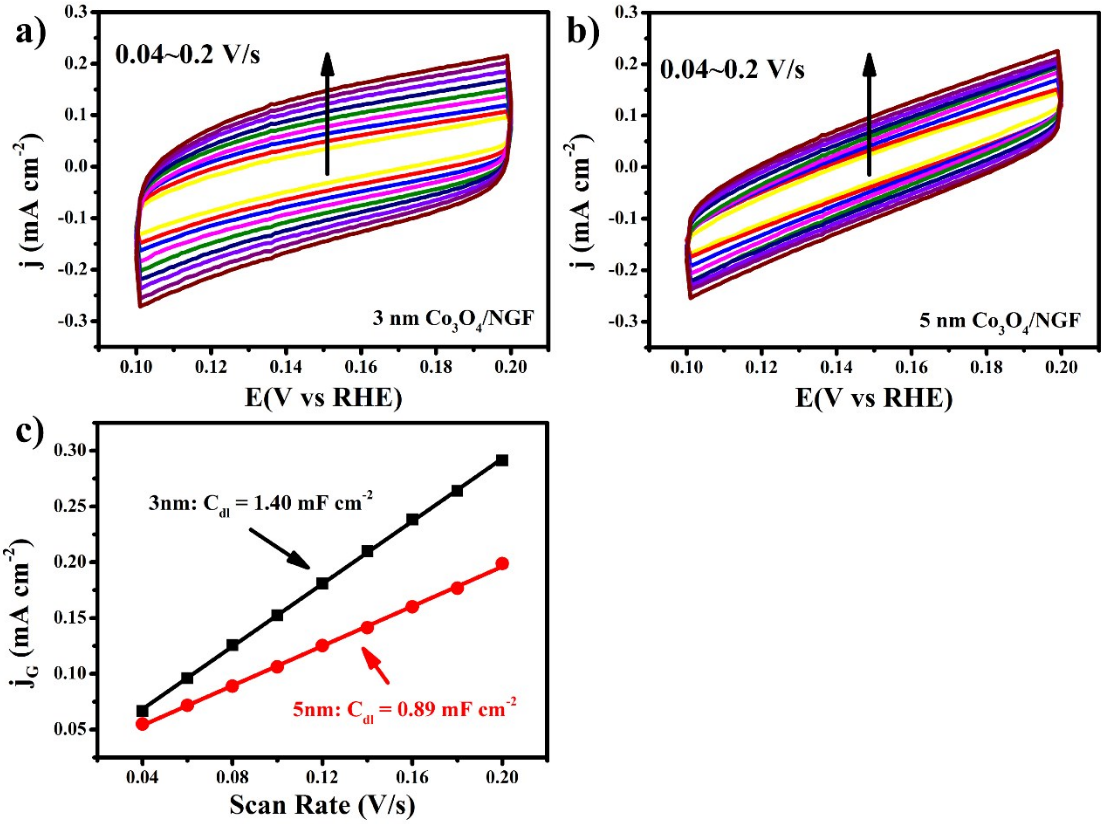

Figure S11. Electrochemical properties of Co_3O_4/NGF in 1M KOH. Cyclic voltammograms in the non-faradaic-voltage range of **a)** 3nm Co_3O_4/NGF and **b)** 5nm Co_3O_4/NGF. **c)** Double-layer charging currents at +0.15 V (vs. RHE) voltage scan rate. Symbols and the line are experimental data derived from a and the linear fit to data, respectively.

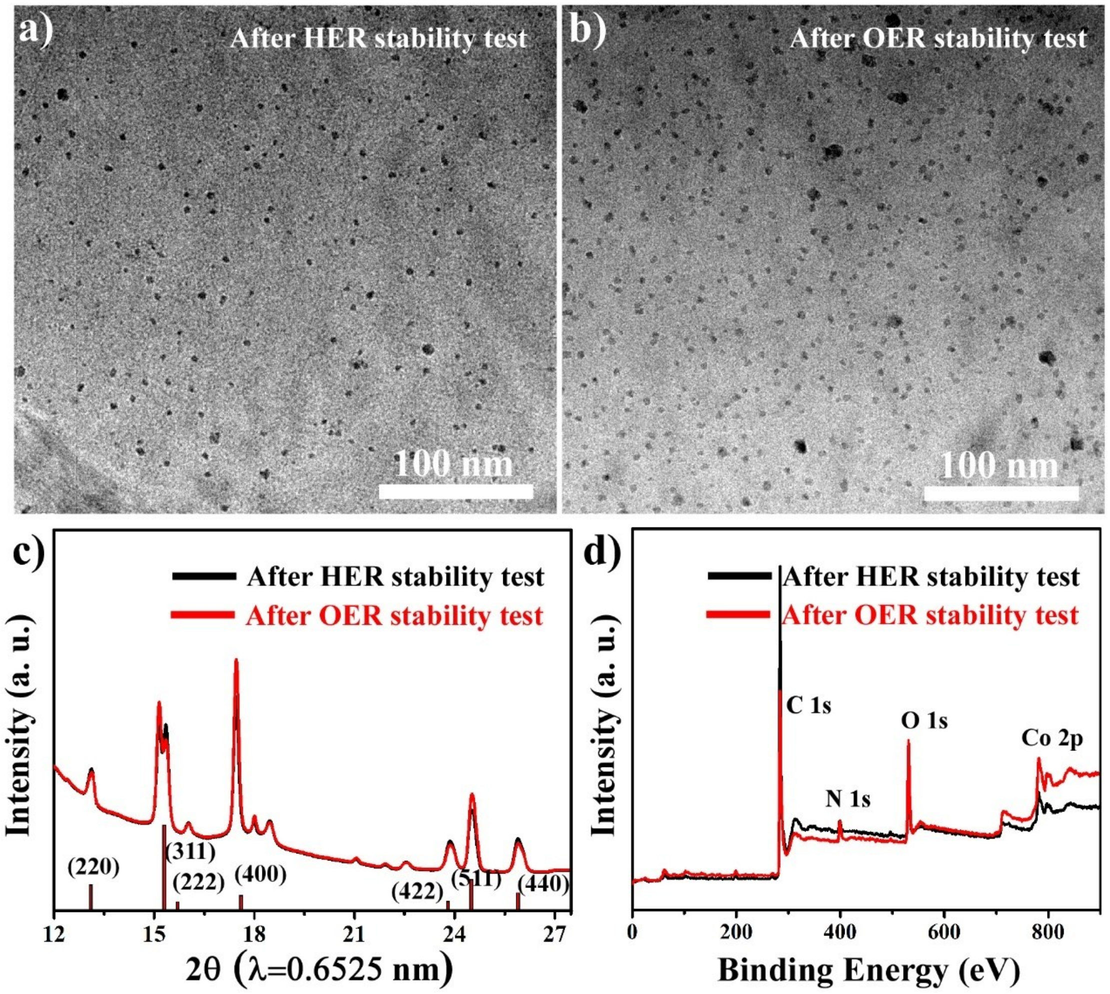

Figure S12. Characterizations of 3 nm Co_3O_4/NGF after 2000 cycles of HER and OER test in 1M KOH). TEM image of Co_3O_4/NGF after **a)** HER and **b)** OER stability tests. (The size of particles in TEM images remains at ~3 nm) **c)** XRD spectrum and **d)** XPS spectrum of Co_3O_4/NGF after HER and OER stability tests.

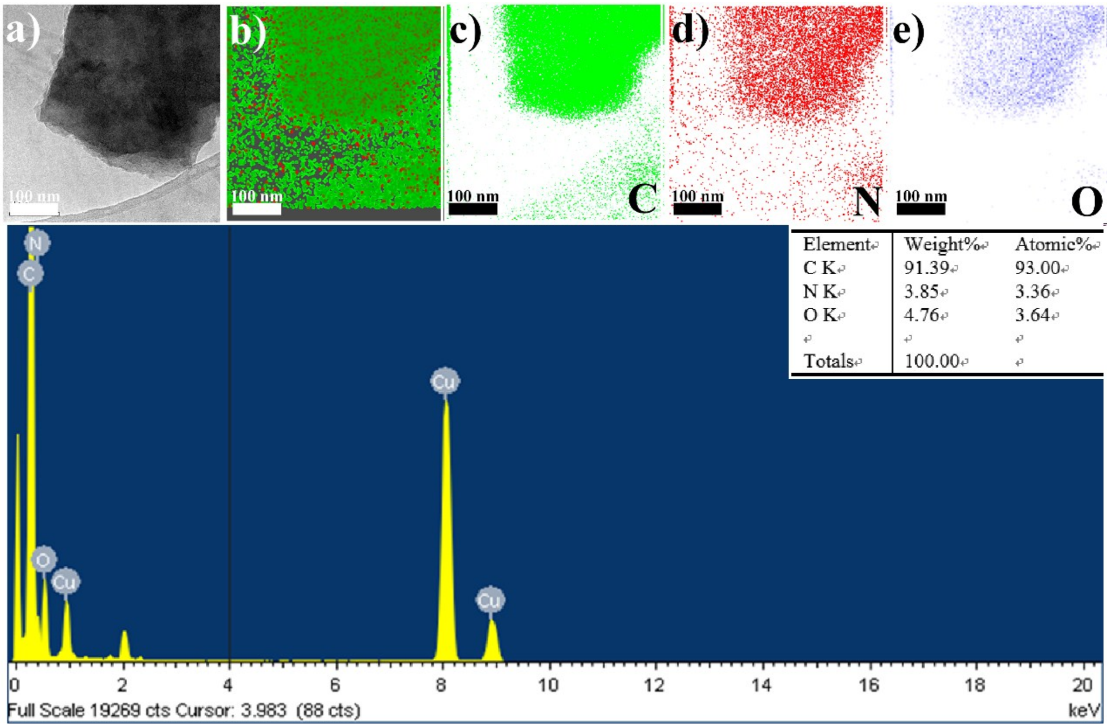

Element	Weight%	Atomic%
C K	91.39	93.00
N K	3.85	3.36
O K	4.76	3.64
Totals	100.00	

Figure S13. TEM elemental mapping results of N-doped Graphene Foam (NGF). a) TEM image of NGF, **b)** Combined mapping image, and **c)** C, **d)** N and **e)** O elemental mapping images of NGF. Followed by the spectrum of C, N and O element content in NGF.

Supporting Tables

Table S1. Selected summary of the HER performance of Cobalt based materials and compared with our work.

Catalyst	Current Density j (mA cm^{-2})	Overpotential at corresponding j (mV)	Tafel slope (mV dec^{-1})	Electrolyte	Ref.
Co_3O_4/NGF (size ~3 nm)	10	191	62	1 M KOH	In this work
	20	233			
	50	300			
Co/NG	10	337	-	0.1 M NaOH	*ACS appl mater & inter.* **2015**, 7, 8083-8087
Co/NC	10	210	108	1 M KOH	*J Mater Chem A.* **2014**, 2, 20067-20074
Co-NC	10	270	131	1 M KOH	*J Mater Chem A* **2016**, 4, 3204-3209.
Co/BCN	10	183	73.2	1 M KOH	*ACS Nano.* **2016**, 10, 684-694
Co-NRCNT	10	370	-	1 M KOH	*Angewandte Chemie,* **2014***,* 126, 4461-4465.
Co-NCNT/CC	10	180	193	1 M KOH	*ChemSusChem,* **2015,** 8, 1850-1855
Co@NCNT	10	244	163	0.1 M KOH	*J.Mater.Chem.A* **2016**,4,17288-17298
Co/N-doped CNT	10	240	85	1 M KOH	*Nanoscale,* **2015***,* 7, 2306-2316
CoP/rGO	10	209	129	1 M KOH	*J. Am. Chem. Soc.* **2014**, 136, 7587-7590

Table S2. Selected summary of the OER performance of Cobalt based materials and compared with our work.

Catalyst	Current Density j (mA cm^{-2})	Overpotential at corresponding j (mV)	Tafel slope (mV dec^{-1})	Electrolyte	Ref.
Co_3O_4/NGF (size ~3 nm)	10	311	72	1 M KOH	In this work
	20	332			
	50	371			
Co-NC	10	370	76	1 M KOH	*J. Mater. Chem. A* **2016**, 4, 3204-3209.
Co-P	10	345	47	1 M KOH	*Angew. Chem. Int. Ed.,* **2015***,* 54, 6251-6254
Co@NCNT	10	461	116	1 M KOH	*J. Mater. Chem. A* **2016**,4,17288-17298
Co NPs	10	400	-	0.1 M KOH	*J. Am. Chem. Soc.* **2015***,* 137, 7071−7074
Co@N-C	10	400	-	1 M KOH	*J. Mater. Chem. A.* **2014**, 2, 20067-20074
N/Co-doped PCP//NRGO	10	430	-	0.1 M KOH	*Adv. Funct. Mater,* **2015**, 25, 872-882.
Co-P/NC	10	319	52	1 M KOH	*Chem. Mater* **2015**, *27*, 7636-7642.
Co phosphide/phosphate thin film	30	330	65	1 M KOH	*Adv. Mater.* **2015**, *27*, 3175-3180
CoP/NG	20	300	54	1 M KOH	*Nanoscale*, **2016**,8, 10902-10907
CoP NWs	10	320	64	1 M KOH	*Green Chem.* **2016**, 18, 1459-1464
CoP/rGO	10	340	66	1 M KOH	*Chem. Sci.* **2016**, 7, 1690-1695
	20	379			

Table S3. Selected summary of the overall water-splitting performance of Cobalt based materials and compared with our work.

Catalyst	Current Density j (mA cm^{-2})	(V)	Electrolyte	Ref.
Co_3O_4/NGF (size ~3 nm)	10	1.63	1 M KOH	In this work
	20	1.69		
	40	1.78		
Co-NC	10	1.64	1 M KOH	*J Mater Chem A* **2016**, 4, 3204-3209.
Co-P	10	1.67	1 M KOH	*Angew. Chem. Int. Ed.,* **2015**, 54, 6251-6254
Co-P/NC	10	1.69	1 M KOH	*Chem Mater* **2015**, 27, 7636-7642.
CoP/NG	10	1.58	1 M KOH	*Nanoscale*, **2016**,8, 10902-10907
Co(OH) 2 @PANI Co(OH) 2 @PANI CoMnO@CN	54	1.70	1 M KOH	*J. Am. Chem. Soc.* **2015**, 137, 14305-14312
	108	1.80		
CoP/rGO	10	1.70	1 M KOH	*Chem. Sci.* **2016**, 7, 1690-1695

Table S4. Summarize data on Co_3O_4 nanoparticles with different diameters on N-doped graphene foam. Noted that the diameter data was statistically obtained from TEM results and elemental content data derived from XPS results.

Concentration of $CoCl_2$ (mol/L)	Diameter of Co_3O_4 nanoparticles (nm)	Co (Atom %)	O (Atom %)	N (Atom %)	C (Atom %)
0	0	0	3.53	3.45	93.02
0.02	2.9±0.3	1.7	5.8	3.1	89.4
0.05	5.0±0.2	2.7	7.5	3.0	86.8
0.1	10.3±0.4	4.3	10.4	3.5	81.8
0.2	14.8±0.2	5.4	11.8	3.6	79.2
0.5	21.0±0.2	7.8	13.7	3.4	75.1

References

1. J. W. Nichol, S. T. Koshy, H. Bae, C. M. Hwang, S. Yamanlar and A. Khademhosseini, *Biomaterials*, 2010, **31**, 5536-5544.
2. Z. Chen, W. Ren, L. Gao, B. Liu, S. Pei and H. M. Cheng, *Nat. Mater.*, 2011, **10**, 424-428.
3. K. Vanommeslaeghe, E. Hatcher, C. Acharya, S. Kundu, S. Zhong, J. Shim, E. Darian, O. Guvench, P. Lopes, I. Vorobyov and A. D. MacKerell, *J. Comput. Chem.*, 2010, **31**, 671-690.
4. K. Vanommeslaeghe and A. D. MacKerell, *J. Chem. Inf. Model*, 2012, **52**, 3144-3154.
5. W. Humphrey, A. Dalke and K. Schulten, *J. Mol. Graph. Model.*, 1996, **14**, 33-38.
6. J. C. Phillips, R. Braun, W. Wang, J. Gumbart, E. Tajkhorshid, E. Villa, C. Chipot, R. D. Skeel, L. Kale and K. Schulten, *J. Comput. Chem.*, 2005, **26**, 1781-1802.
7. L. Wu and M. Z. Liu, *Carbohyd. Polym.*, 2008, **72**, 240-247.